Available online at www.sciencedirect.com
SCIENCE DIRECT®

Journal of the European Ceramic Society 23 (2003) 1743–1750
www.elsevier.com/locate/jeurceramsoc

Wear properties of Y–α/β composite sialon ceramics

Mark I. Jones[a,*], Kiyoshi Hirao[a], Hideki Hyuga[b], Yukihiko Yamauchi[a], Shuzo Kanzaki[a]

[a]*Synergy Materials Research Center, AIST, 268-1 Shimo-shidami, Nagoya 463-8687, Japan*
[b]*Fine Ceramics Research Association, 268-1 Shimo-shidami, Nagoya 463-8687, Japan*

Received 12 June 2002; received in revised form 21 October 2002; accepted 2 November 2002

Abstract

The tribological properties of yttrium containing α/β composite sialon ceramics have been studied under non-lubricated conditions by means of block-on-ring and ball-on-disk type experiments against a commercial silicon nitride material. The sialon ceramics were produced by hot pressing powder mixtures of Si_3N_4, AlN, Al_2O_3 and Y_2O_3, resulting in composite ceramics containing different amounts of the α/β phases. The effects of microstructural differences on the mechanical properties of the ceramics, and their wear characteristics under a range of testing conditions have been assessed. It was found that Vickers hardness decreased whilst both fracture toughness and bending strength increased with increasing amount of β phase in the composite. Under mild testing conditions, material removal was considered to occur by polishing of the surface, and in this case the high α-sialon composites exhibited the highest wear resistance, reflecting their higher hardness. Under severe testing conditions, the wear behaviour was characterised as microcracking caused by the higher Hertzian stress levels, and resulted in grain removal or "dropping" from the surface of the materials. Under these conditions, the elongated microstructure and higher fracture toughness of the low α-sialon composites hinder the crack propagation and result in better wear characteristics when compared to the fine equiaxed α-sialon materials.

Keywords: Ball-on-disk; Block-on-ring; Microstructure; Sialons; Testing; Wear resistance

1. Introduction

Ceramic materials have long been promoted as promising materials for use in tribological applications, due to their high hardness, high temperature stability and chemical inertness relative to metals. Amongst the advanced engineering ceramics silicon nitride is recognised as one of the most suitable candidates for these applications due to its unique combination of strength and toughness.[1] Silicon nitride exists in two crystal structure modifications, α and β, with the β phase being stable at higher temperatures. The microstructures of the two phases are distinctly different; α Si_3N_4 ceramics have a uniform equiaxed microstructure whereas the anisotropic growth rates in β Si_3N_4 result in a microstructure containing elongated β grains in a fine grained matrix. The differences in crystal structure and microstructure result in a range of ceramics with a wide range of mechanical properties; α Si_3N_4 possesses higher hardness than β Si_3N_4, but the growth of the elongated β grains is a prerequisite for achieving ceramics with high toughness.[2]

The covalent bonding of this ceramic makes the production of fully dense bodies virtually impossible without the use of metal oxides to aid sintering, and the use of these additives results in a Si_3N_4 matrix surrounded by a grain boundary phase, which is usually amorphous. The properties of the materials are therefore not solely determined by the microstructure and morphology of the silicon nitride grains, but also by the nature of this residual grain boundary phase. There have been numerous studies on the effect of grain boundary composition on the mechanical properties of silicon nitride ceramics,[3,4] and also reports of improved mechanical properties through crystallisation of the grain boundary phase.[5]

Both the α and the β phases of Si_3N_4 can form substitutional solid solutions with the Si and N elements being replaced with Al and O, respectively. The two resulting phases are termed α- and β-SiAlON respectively. In addition, the α-sialon phase can incorporate rare earth metallic elements within its structure, and sintering of these materials occurs through the forma-

* Corresponding author. Tel.: +81-52-739-0133; fax: +81-52-739-0136.
E-mail address: mark.jones@aist.go.jp (M.I. Jones).

0955-2219/03/$ - see front matter © 2003 Elsevier Science Ltd. All rights reserved.
PII: S0955-2219(02)00401-6

tion of a transient liquid phase which results in ceramics with reduced amounts of residual glassy phase.[6]

The response of a material in tribological applications is not an inherent material property but depends to a great degree on experimental conditions such as sliding velocity and normal load, as well as environmental conditions such as temperature and humidity. For this reason, research has generally focussed on producing "wear maps" [7] and "wear transition diagrams" [8] in an attempt to identify the wear mechanisms operating over a wide range of conditions. Numerous assessments of the wear characteristics of silicon nitride ceramics have been carried out, and include investigations into the effects of sliding speed [9] temperature [10] and humidity.[11] The wear modes occurring in silicon nitride depend to a large degree on these testing conditions, and under low loads and relatively low temperatures, the wear mode is one which is to a large part controlled by tribochemical reactions. Under these conditions, reaction between the sliding surface and water vapour in the air results in the formation of an amorphous $Si(OH)_4$ layer, and wear is determined by the rate of formation and removal of this film.[8] Under higher loads, the dominant wear mechanism in one of mechanical wear, occurring by the propagation of cracks along grain boundaries, and resulting in micro fracture within the material 12 In this regime the microstructure of the material is expected to play a more significant role in wear than its chemical stability, and recently, there have been studies carried out to assess the effects of microstructure on wear, although these have concentrated on factors such as grain size and amount of grain boundary phase,[13] and microstructure anisotropy.[14] However, despite the fact that the importance of microstructure, in terms of the relative amounts of the α and β phases, on the mechanical properties of silicon nitride and sialon materials is well documented,[15,16] there are relatively few studies on the effects of these factors on the wear properties.[17,18] In this work, we report on the effect of the composition of mixed α/β composite sialon ceramics on their mechanical and tribological properties. Wear properties were assessed under non-lubricating conditions over a range of normal loads and employing both block-on-ring and ball-on-disk experiments.

2. Experimental

2.1. Sample preparation

The compositions of the starting materials were all within the Y containing α-sialon plane as shown in Fig. 1. Within this plane the nominal composition can be given by $Y_{m/3}Si_{12-(m+n)}Al_{m+n}O_nN_{16-n}$. Two of the composites produced were Y-α-sialon/β-sialon composites with compositions lying on the Si_3N_4-9AlN·Y_2O_3 line. The other two composites were produced from compositions within the single phase α-sialon region of this plane. The samples were produced by mixing appropriate amounts of α-Si_3N_4 (E-10 grade, Ube Industries, Ltd., Japan), Al_2O_3 (AKP-50, Sumitomo Chemical Co., Ltd., Japan), AlN (F grade, Tokuyama Co., Japan) and Y_2O_3 (RU-P, Shin-Etsu Chemical Co., Ltd., Japan) in methanol, using a Si_3N_4 pot and Si_3N_4 balls. The slurry was dried, and then passed through 125 mesh. The powders were hot-pressed at 1800 °C for 1 h with an applied pressure of 40 MPa, under a 0.1 MPa nitrogen atmosphere.

2.2. Characterisation

Phase identification was carried out by X-ray diffractometry of crushed samples, and the relative amounts of α and β phases calculated following the method of Gazzara and Messier.[19] For mechanical property measurements, test bars were cut from the sintered specimens, before being ground, and final polished with a 0.5 μm diamond slurry to dimensions of 3×4×40 mm. Additional samples for block-on-ring tests were machined in the same way to a size of 3×4×1.5 mm thickness, and those for ball-on-disk type experiments were actually in the form of rectangular plates 27×30×4 mm thickness. For all mechanical and wear property analyses, the samples were tested on the face normal to the hot pressing direction. Fracture surfaces of the samples following bending strength tests were observed by scanning electron microscopy, SEM (JSM-6340F, Jeol Ltd., Japan).

Strength measurements were carried out by four-point bend with inner and outer spans of 10 and 30 mm, respectively. Young's modulus was measured by the Pulse Echo method and Vickers hardness tests were carried out under a load of 98 N. Fracture toughness (K_{IC}) was determined by the indentation-fracture (IF) method under the same load. The oxidation kinetics of the samples was studied by thermogravimetry. Samples

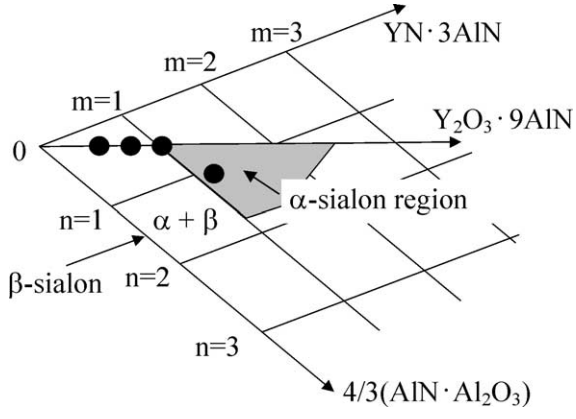

Fig. 1. Starting compositions of the materials in the α-sialon plane.

Table 1
Sample designations and compositions

Sample	*m*	*n*	Theoretical phase structure	Phases identified by XRD	Calculated β content (%)
1	1.1	1.1	α-Sialon	α-Sialon	0
2	1.0	0.5	α-Sialon	α-Sialon + β sialon (trace)	3
3	0.70	0.35	α-Sialon + β sialon	α-Sialon + β sialon	25
4	0.50	0.25	α-Sialon + β sialon	α-Sialon + β sialon	49

Sample 2 showed trace amounts of β-sialon, reflecting the composition of this sample on the boundary of the α-sialon phase region (see Fig. 1).

of the sintered bodies were heated to 1200 °C at a heating rate of 10 °C min^{-1} in an atmosphere of dry air with a flow rate of 100 ml min^{-1}, and the mass change due to oxidation was monitored continuously over a holding period of 50 h at the set temperature.

2.3. Wear tests

Block-on-ring tests were carried out under non-lubricated conditions using the equipment described in a previous paper.[14] Briefly, the sialon samples were employed as the blocks and were located in a holder above the ring, which was a commercially available silicon nitride material (SN235P, Kyocera, Japan) of 30 mm diameter. The surface roughness of both the Si_3N_4 ring and the sialon specimens were prepared under Rz 0.1 μm. Temperature and humidity were kept constant at 25±3 °C, 25±2% RH. Sliding speed and distance were kept constant at 0.15 m/s and 75 m, respectively, and tests were conducted with normal loads varying from 5 to 90 N. The worn volume of the sialon blocks was calculated by integration of the sectional worn area measured by a contact type roughness tester (SV-624, Mitsutoyo, Japan). The worn area was measured at nine equi-distant points (spacing 0.3 mm) in the direction parallel to the sliding direction.

For ball-on-disk type tests the sialon plates were rotated against a stationary Si_3N_4 ball with a diameter of 10 mm at a load of 49 N and a speed of 0.18 m/s. The sliding distance was 108 m, and the other conditions were the same as those in block-on-ring tests. For the worn plate specimens, the cross sectional area of the worn track was taken as the average of that measured at four separate locations. The worn volume was calculated according to Japanese Industrial Standard (JIS R1613) by the following equation

$$\text{Worn volume} = (\pi R(S_1 + S_2 + S_3 + S_4))/2$$

where R and S are the sliding radius and cross section area of the worn track.

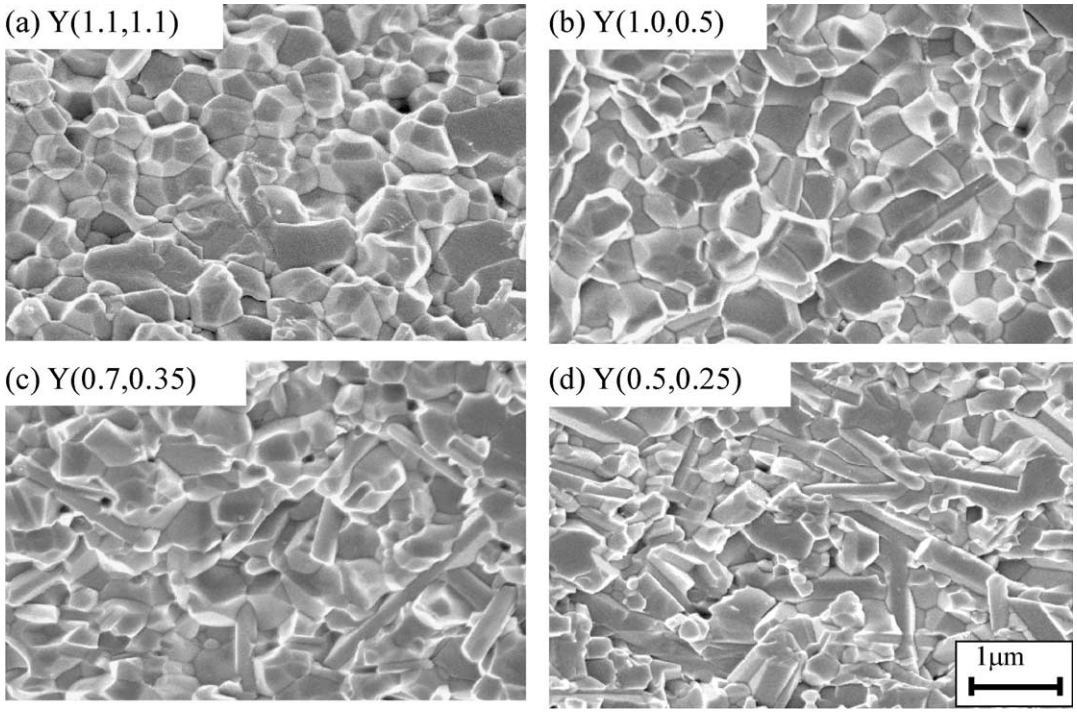

Fig. 2. Fracture surfaces of the sintered sialon composites. The α-sialons show an equiaxed microstructure (a and b) whilst the number of elongated grains increases with β-Sialon content (c and d).

3. Results and discussion

All of the samples were sintered to full density (>98% theoretical density). Table 1 shows the designations of the samples and the phases identified by XRD, along with the calculated β content. Sample 1 (Y-1.1,1.1) was single phase α-sialon whilst sample 2 (Y-1.0,0.5) contained trace amounts of β-sialon, reflecting its composition lying on the boundary of the α-sialon phase field (Fig. 1). Samples 3 and 4 (Y-0.7,0.35 and Y-0.5,0.25) were composite materials containing both α-and β-sialon phases. The fracture surfaces of the samples following bending tests are shown in Fig. 2. The microstructure of the α-sialon samples (Fig. 2a and b) comprised uniform equiaxed grain morphology with average grain size of approximately 0.5–1.0 μm. The composite sialons (Fig. 2c and d) exhibited a bimodal microstructure where elongated β grains of a few microns in length and submicron diameters were dispersed in a matrix of fine α-sialon grains. These differences in microstructure are reflected in the mechanical properties of the samples as shown in Fig. 3. The α-sialons exhibited the highest hardness, reflecting the inherently higher hardness of the alpha phase, and the equiaxed microstructure of these materials, and there was a decrease in hardness with increasing β content. However, both fracture toughness and bending strength increased monotonically with increasing β content. The higher fracture toughness and strength of the α/β composites is due to the presence of the elongated β grains within the microstructure, which facilitate toughening mechanisms such as crack bridging, as is commonly observed in "in-situ" toughened silicon nitride ceramics.[20] Despite the difference in phase composition of the materials, the Young's modulus of the samples appeared to show little dependence, and for all four samples was in the region of 320±5 GPa.

A wear diagram indicating the relationship between the composition, normal load and worn volume of the samples following the block-on-ring wear tests is given in Fig. 4. As can be seen in this figure, at low normal loads during block-on-ring experiments (5 and 30 N), the composite samples with the high β content showed appreciably more wear than the α sialon samples. As the load was increased to 90 N (the maximum obtainable with the current experimental equipment) this trend was reversed, with the α/β composites showing slightly better wear properties than the single-phase materials. This trend is further highlighted with the results from the ball-on-disk experiment, also shown in Fig. 4, where the α-sialons show an order of magnitude higher wear than the composites. The worn surfaces of the α-sialon (sample 1) and the α/β composite (sample 4) specimens following Block-on-Ring wear tests at a normal load of 5N are shown in Fig. 5. In both cases the surfaces were relatively smooth and showed no evidence of appreciable material removal (Fig. 5a and b). Scattered very fine particles and partially agglomerated material could be seen on the worn surfaces. The smooth appearance of the surfaces is representative of wear in which no

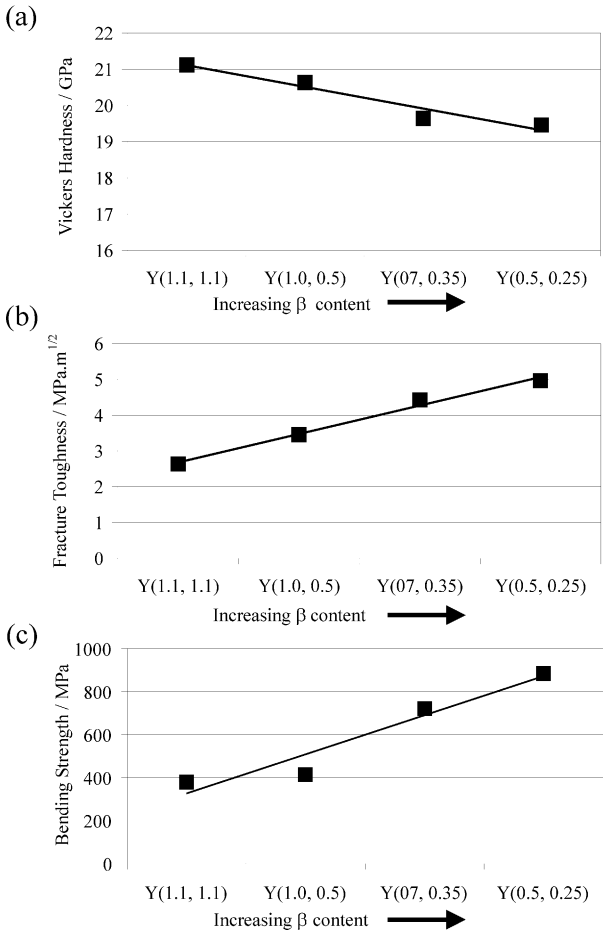

Fig. 3. Mechanical properties of the composite sialons: (a) hardness, (b) fracture toughness and (c) bending strength.

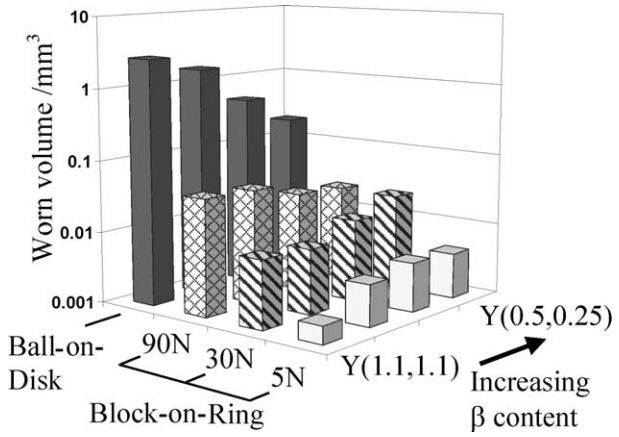

Fig. 4. Wear map showing the relationship between composition, normal load and worn volume of sialon block specimens obtained from the block-on-ring tests, along with the result from the ball-on-disk test.

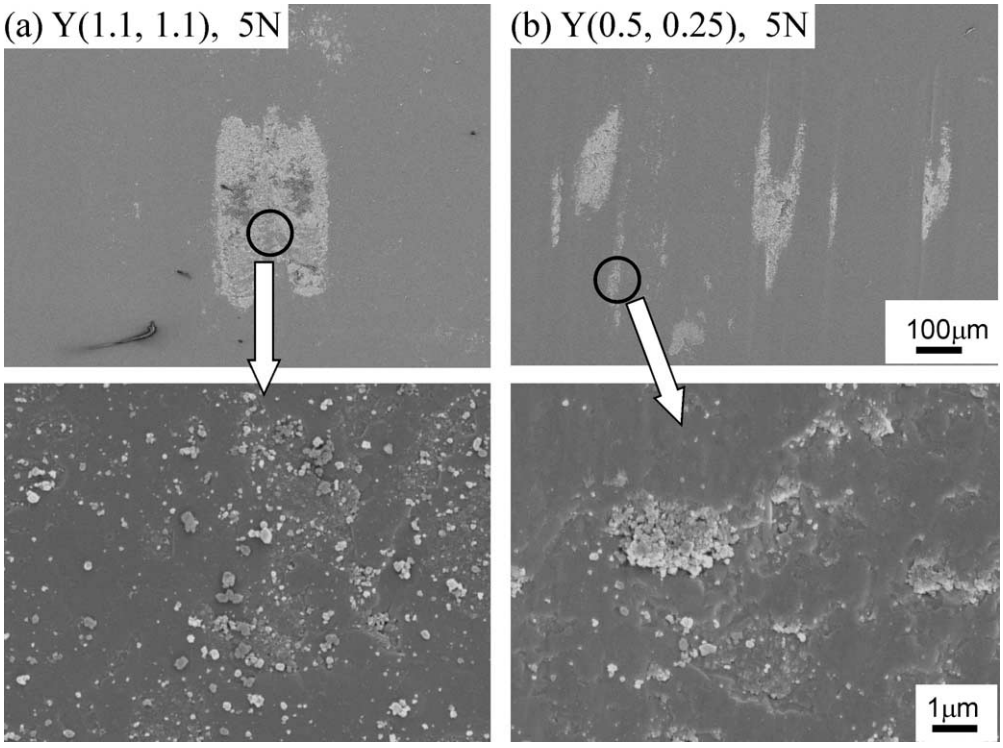

Fig. 5. Worn surfaces of (a) the α-sialon and (b) α/β composite samples following block-on-ring experiments at 5 N. Both surfaces are relatively smooth with no obvious signs of material removal. The α-sialon surface was worn less than the composite due to its higher hardness.

microcracking occurs in the material, and the wear mode is predominantly controlled by tribochemical reactions. Gomes et al. reported that the polished appearance of a worn silicon nitride was due to a combination of fine abrasion modes and humidity-assisted tribo-oxidation.[21] Under these conditions, the higher hardness of the fine grained α-sialons imparts greater resistance to material removal. It is generally accepted that in ceramic materials, this type of worn surface is characterised by localised plastic flow and tribochemical reactions.[22] These tribochemical reactions, which are stimulated by friction, can result in the formation of a reaction layer, which can reportedly lower the wear rate in humid environments.[23] However, other authors have reported that such reaction layers play no role in reducing wear.[10] In silicon nitride based ceramics, the tribochemical reaction results in the formation of a silica layer, and it is therefore expected that the propensity to oxidation of the material will have a bearing on the formation of such layers.

The TG data of the full alpha and the high beta samples following 50 h at 1200 °C showed that the weight gain was 0.19 and 1.65 mg cm^{-2}, respectively. That is, the high beta composite showed an order of magnitude greater weight gain than that of the full alpha. It is generally reported that the oxidation resistance of alpha sialons is superior to that of beta sialon, due to the reduced amount of glassy phase in the former.[24,25] This greater resistance to oxidation in the case of the alpha sample may be another reason for the improved wear behaviour under low loads. Andersson et al reported that during unlubricated sliding of self mated Si_3N_4, high local temperatures at the asperity contacts resulted in oxidation and easily detachable reaction products.[26] The greater propensity to oxidation for the high beta composite may lead to increased wear through the removal of the oxide film by adhesive wear, and thus exposing the surface to further oxidation. High wear rates by such oxidation mechanisms have been reported for high temperature sliding of silicon nitride, where oxidation is the dominant wear mechanism.[8]

As the normal load is increased, the wear conditions become more severe, and in silicon nitride ceramics it has been shown that under high stress or high load conditions the predominant wear mode is one where wear occurs by the propagation of cracks along the grain boundaries leading to microfracture.[27] Such intergranular cracking can lead to the "pulling out" or "dropping" of grains from the material surface.[28] Worn surfaces following block-on-ring tests at a normal load of 90 N are shown in Fig. 6. For both the α-sialon and the α/β composite, the surfaces were very rough and high magnification revealed that the microstructure was clearly visible in areas where grains had been removed from the surface. This is most clearly seen for the α-sialon sample (Fig. 6a). Analysis of the Hertzian stress fields produced during the wear tests, using the method described by Kaoki et al.,[29] indicated maximum tensile

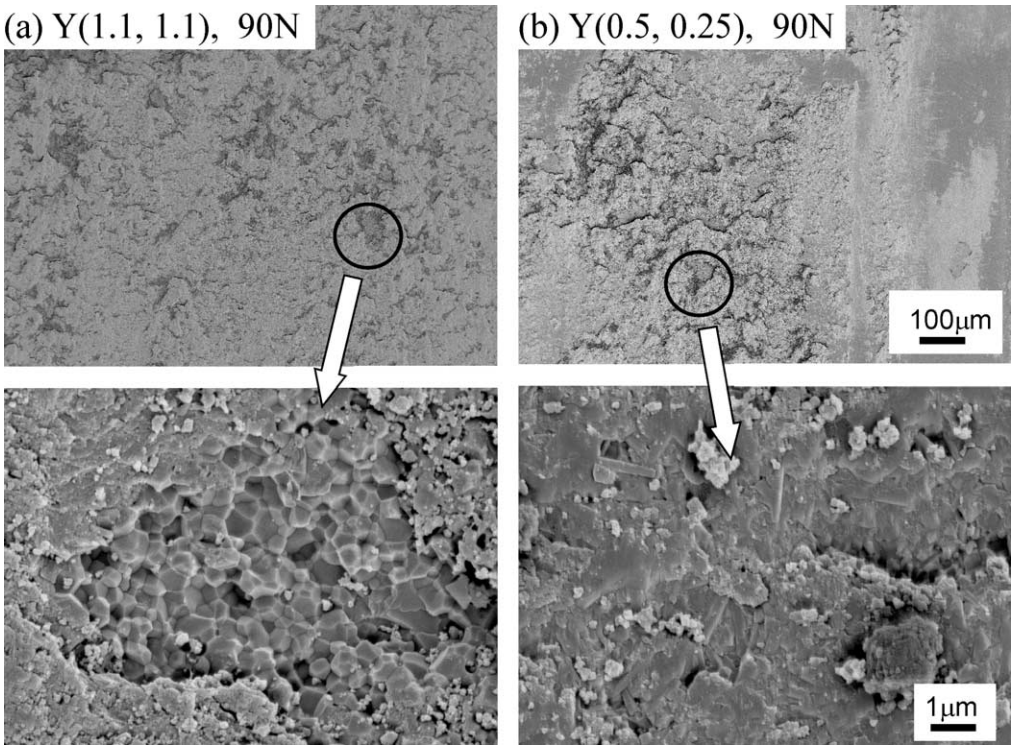

Fig. 6. Worn surfaces of (a) the α-sialon and (b) α/β composite samples following block-on-ring experiments at 90 N. The worn surfaces are very rough and areas of exposed microstructure can be observed due to grain dropping. This phenomena was more prevalent for the fine grained α-sialon.

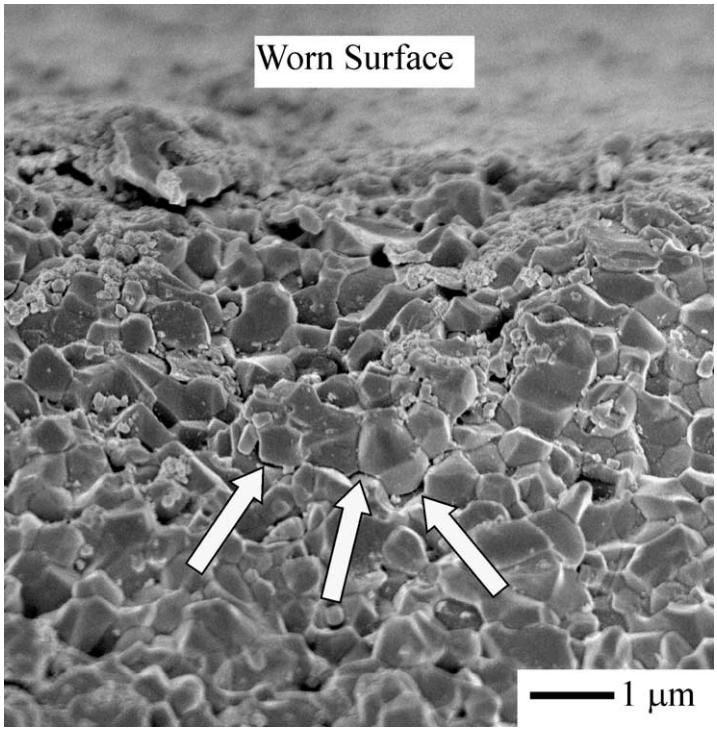

Fig. 7. Fracture surface of the Y(1.1,1.1) sample following ball-on-disk wear test. Many grain boundary microcracks can be observed beneath the worn surface (indicated by arrows).

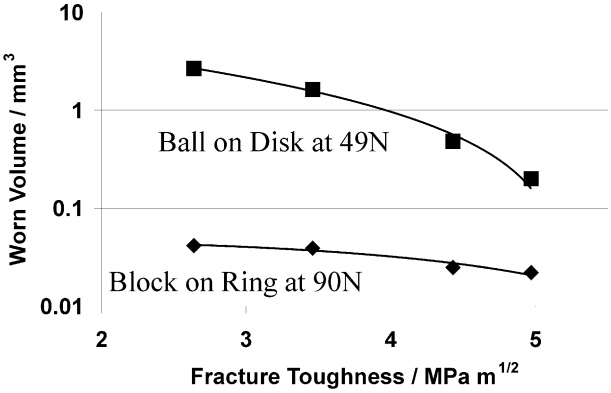

Fig. 8. Worn volume of the samples plotted against fracture toughness.

stresses of approximately 85, 190 and 370 MPa for the block-on-ring tests at normal loads of 5, 30 and 90 N, respectively. For the ball-on-disk wear tests the same analysis yields a maximum tensile stress one order of magnitude higher, approximately 2.2 GPa. It should be noted that the stress level for the block-on-ring test at 90 N is comparable to the bending strength of the two α-sialon materials, and that for the ball-on-disk test is higher than the strength of all four samples. Under these conditions, the dropping of grains is thought to occur following microcracking within the specimen due to the high tensile stresses produced.[30] Fig. 7 shows the fractured surface of the Y(1.1, 1.1) specimen following the ball-on-disk wear test. In this figure, the sample is shown fractured in the direction normal to both the worn surface and the sliding direction. The concave region beneath the worn surface shows the generation of many grain boundary microcracks, and it is thought that the presence of these cracks leads to the removal of individual grains from the surface of the material during wear under severe conditions. Under these conditions, the improved fracture toughness in the composite materials, afforded by the presence of the elongated β grains, makes the propagation of these cracks more difficult, and consequently the wear of these materials is reduced in comparison to the fine grained α-sialons. The worn volume of the samples is plotted against their fracture toughness in Fig. 8. It can be seen that the wear decreased with increasing fracture toughness of the samples, and that this phenomenon was more pronounced for the samples tested under the more severe conditions of the ball-on-disk experiments.

4. Conclusions

The mechanical and wear properties of mixed α/β sialon composite ceramics with various ratios of α and β phases, have been examined under a range of testing conditions. It was found that with increasing β content in the composites, there was a decrease in hardness, but a monotonic increase in both bending strength and fracture toughness due to the presence of elongated grains in the microstructure. In block-on-ring experiments at low loads, the wear behaviour was characterised as one controlled mainly by tribochemical reactions and microabrasion. Under these conditions, the higher hardness of the single-phase α-sialon materials results in the best wear properties. The propensity for easier oxidation in the α/β composites materials may also contribute to greater wear through the removal of the oxide film by adhesive wear.

However under heavier normal loads, and under ball-on-disk experiments, where higher Hertzian stress fields are generated, the wear mode changes to one where wear occurs by the removal of individual grains following microcracking within the grain boundary phase. Under these conditions, the fracture toughness of the material has a significant effect on crack propagation and the bimodal microstructure of the α/β composites results in improved wear properties.

Acknowledgements

The authors are indebted to Dr. Shuji Sakaguchi of AIST, Japan, for the stress analysis calculations.

References

1. Hoffmann, M. J. and Petzow, G., Microstructural design of Si_3N_4 based ceramics. *Mat. Res. Soc. Proc*, 1993, **287**, 3–14.
2. Becher, P. F., Hwang, S. L., Lin, H. T. and Tiegs, T. N., Microstructure contributions to the fracture resistance of silicon nitride ceramcs. In *Tailoring of Mechanical Properties of Si_3N_4 Ceramics*, ed. M. J. Hoffmann and G. Petzow. Kluwer Acad Press, Netherlands, 1994, pp. 87–100.
3. Lu, H.-H. and Huang, J.-L., Effect of Y_2O_3 and Yb_2O_3 on the microstructure and mechanical properties of silicon nitride. *Ceram. Int*., 2001, **27**, 621–628.
4. Sun, E. Y., Becher, P. F., Plucknett, K. P., Hsueh, C.-H., Alexander, K. B., Waters, S. B., Hirao, K. and Brito, M. E., Microstructural design of silicon nitride with improved fracture toughness: II, Effects of yttria and alumina additives. *J. Am. Ceram. Soc*., 1998, **81**(11), 2049–2831.
5. Cinibulk, M. K., Thomas, G. and Johnson, S. M., Fabrication and secondary-phase crystallisation of rare-earth disilicate-silicon nitride ceramics. *J. Am. Ceram. Soc*., 1992, **75**(8), 2037–2043.
6. Campbell, P., Laoui, T., Celis, J. P. and Van Der Biest, O., The influence of intergranular phases on the tribological performance of sialons. *Mat. Sci. Eng*., 1996, **A207**, 72–86.
7. Adachi, K., Kato, K. and Chen, N., Wear map of ceramics. *Wear*, 1997, **203-204**, 291–301.
8. Dong, X. and Jahanmir, S., Wear transition diagram for silicon nitride. *Wear*, 1993, **165**, 169–180.
9. Muratov, V. A., Luangvaranunt, T. and Fischer, T. E., The tribochemistry of silicon nitride: effects of friction, temperature and sliding velocity. *Trib. Int*., 1998, **31**(10), 601–611.
10. Skopp, A., Woydt, M. and Habig, K.-H., Tribological behavior of silicon nitride materials under unlubricated sliding between 22 °C and 1000 °C. *Wear*, 1995, **181-183**, 571–580.

11. Gee, M. G. and Butterfield, D., The combined effect of speed and humidity on the wear and friction of silicon nitride. *Wear*, 1993, **162-164**, 234–245.
13. Dogan, C. P. and Hawk, J. A., Microstructure and abrasive wear in silicon nitride ceramics. *Wear*, 2001, **250**, 256–263.
14. Nakamura, M., Hirao, K., Yamauchi, Y. and Kanzaki, S., Tribological properties of unidirectionally aligned silicon nitride. *J. Am. Ceram. Soc*., 2001, **84**(11), 2579–2584.
15. De Arellano-Lopez, A. R., McMann, M. A., Singh, J. P. and Martinez-Fernandez, J., Microstructure and room-temperature mechanical properties of Si_3N_4 with various α/β phase ratios. *J. Mat. Sci*., 1998, **33**(24), 5803–5810.
16. Bandyopadhyay, S., Hoffman, M. J. and Petzow, G., Densification behavior and properties of Y_2O_3-containing α-sialon-based composites. *J. Am. Ceram. Soc*., 1996, **79**(6), 1537–1545.
17. Gomes, J. R., Oliviera, F. J., Silva, R. F., Osendi, M. I. and Miranzo, P., Effect of α-/β Si_3N_4 phase ratio and microstructure on the tribological behaviour up to 700 °C. *Wear*, 2000, **239**, 59–68.
18. Liu, D.-M., Lin, J.-T. and Lee, R. R. R., Erosive wear behaviour in duophase SiAlON composites. *Cer. Int*, 1998, **24**, 217–221.
19. Gazzara, C. P. and Messier, D. R., Determination of phase content of Si_3N_4 by X-ray diffraction analysis. *Cer. Bull*., 1977, **56**(9), 777–780.
20. Becher, P. F., Sun, E. Y., Plucknett, K. P., Alexander, K. B., Hsueh, C. H., Lin, H. T., Waters, S. B., Westmoreland, C. G., Kang, E. S., Hirao, K. and Brito, M. E., Microstructural design of silicon nitride with improved fracture toughness: 1, effects of grain shape and size. *J. Am. Ceram. Soc*., 1998, **81**(11), 2821–2830.
21. Gomes, J. R., Miranda, A. S., Vieira, J. M. and Silva, R. F., Sliding speed-temperature wear transition maps for Si_3N_4/iron alloy couples. *Wear*, 2001, **250**, 293–298.
22. Ravikiran, A. and Jahanmir, S., Effect of contact pressure and load on wear of alumina. *Wear*, 2001, **251**, 980–984.
23. Fischer, T. E. and Tomizawa, H., Interaction of tribochemistry and microfracture in the friction and wear of silicon nitride. *Wear, Fischer, T.E*, 1985, **105**, 29–45.
24. Ekstrom, T. and Nygren, M., Sialon ceramics. *J. Am. Ceram. Soc*., 1992, **75**(2), 259–276.
25. Jiang, X., Baek, Y.-K., Lee, S.-M. and Kang, S.-J., Formation of an α-SiAlON layer on β-SiAlON and its effect on mechanical properties. *J. Am. Ceram. Soc*., 1998, **81**(7), 1907–1912.
26. Andersson, P. and Holmberg, K., Limitations on the use of ceramics in unlubricated sliding applications due to transfer layer formation. *Wear*, 1994, **175**, 1–8.
27. Wang, Y. and Hsu, S. M., Wear and wear transition mechanisms of ceramics. *Wear*, 1996, **195**, 112–122.
28. Park, D.-S., Han, B.-D., Lim, D.-S. and Yeo, I.-W., A study on wear and erosion of sialon-Si_3N_4 whisker ceramic composites. *Wear*, 1997, **203-204**, 284–290.
29. Kakoi, K. and Obara, T., A numerical method for counter-formal rolling contact problems using special boundary element method. *Jpn. Soc. Mech. Eng Int. J*., 1993, **36**(1A), 57–62.
30. Fischer, T. E., Zhu, Z., Kim, H. and Shin, D. S., Genesis and role of wear debris in sliding wear of ceramics. *Wear*, 2000, **245**, 53–60.